JOURNAL OF GEOPHYSICAL RESEARCH, VOL. 104, NO. D24, PAGES 31,173–31,189, DECEMBER 27, 1999

Role of ecosystem dynamics in biosphere-atmosphere interaction over the coastal region of West Africa

Julie E. Kiang and Elfatih A. B. Eltahir

Department of Civil and Environmental Engineering, Massachusetts Institute of Technology Cambridge

Abstract. In this study, we develop a one-dimensional model of the tropics which includes two-way interaction between the biosphere and the atmosphere, including ecosystem dynamics. The model integrates an atmospheric model, a biospheric model, and a monsoon circulation model and is applied to coastal West Africa to test the sensitivity of the coupled system to changes in vegetation cover. We perform three sets of simulations: one with a fixed monsoon circulation, one with an interactive monsoon circulation, and one with modified boundary conditions at the northern edge of the domain. Our control simulations show that the model is able to reasonably approximate observed conditions. The model simulates a single stable forest equilibrium in the first two sets of simulations, those which correspond most readily with present conditions in West Africa. These simulations indicate that the monsoon plays an important role in modulating the climate of the region and in shaping the response of the system to vegetation changes. Changes in the monsoon which allowed hot and dry air to penetrate into the model domain from the north strongly modified the equilibrium climate toward drier conditions. This finding motivated further testing of the system assuming degraded conditions to the north, which revealed the possibility of two different equilbria: one forest and one grassland. The existence of multiple equilibria in the biosphere-atmosphere system depends not only on the magnitude of the vegetation-induced climate perturbation but also on whether or not the perturbation extends across the threshold in moisture conditions controlling competition between trees and grasses.

1. Introduction

Since prehistoric times, humans have been altering the Earth's environment to make it more hospitable for daily life, to obtain necessary food and shelter, and more recently, to extract economic gain from its vast resources. Over the past few centuries, particularly within the previous few decades, rapid population growth and technological advances have encouraged swifter and more dramatic changes to natural conditions. These human-wrought changes to the Earth have become the subject of great controversy and, to some, cause for great alarm. In particular, numerous studies [e.g., *Lean and Rowntree,* 1997; *Henderson-Sellers et al.,* 1993; *Dickinson and Kennedy,* 1992] have suggested that rapid deforestation in the tropics may significantly impact the regional and global climate. In the face of this concern a thorough understanding of the natural interactions between the biosphere and the atmosphere is warranted, as it can allow us to better manage the Earth's resources for future as well as current generations.

Vegetation can have a strong impact on local and regional climate by affecting the water and energy exchange between the land surface and the atmosphere. Vegetation affects the net radiation, the vertical heat flux from the land surface, and the moist static energy in the boundary layer [*Eltahir,* 1996]. In turn, local atmospheric conditions affect the types of vegetation which exist in a particular location as different plants have different tolerances for heat, moisture, and light availability and different strategies for competition when these resources are scarce. This two-way interaction between the biosphere and the atmosphere determines the equilibrium state of vegetation and climate for a given region.

Speculations on the importance of interactions between the biosphere and the atmosphere began centuries ago. It is said that Christopher Columbus noted a decrease in rainfall on the Canary Islands and in the Azores following deforestation, and attributed high rainfall in the West Indies to the existence of forests there [*Meher-Homji,* 1988]. More recently, scientific research has led to improved understanding

Paper number 1999JD900978.
0148-0227/99/1999JD900978$09.00

of the role of the biosphere in determining atmospheric conditions. Numerous modeling studies of Amazonian deforestation, for example, have consistently shown that large-scale deforestation results in a warmer and drier climate in the deforested tropical region [e.g., *Lean and Warrilow,* 1989; *Shukla et al.,* 1990; *Dickinson and Kennedy,* 1992; *Eltahir and Bras,* 1994]. Using a two-dimensional, zonally symmetric model, *Zheng and Eltahir* [1998] showed that vegetation conditions can affect the dynamics of the West African monsoon. However, these studies consider only a one-way interaction between the biosphere and the atmosphere. Each treats vegetation as a static property of the land surface and examines the differences between the atmospheric climates simulated when either grassland or forest dominates the land surface. However, grasslands are not allowed to evolve into forests, or vice versa, despite climatic conditions which may or may not favor that evolution.

Recent modeling studies have attempted to include two-way interaction between the biosphere and the atmosphere. Among the earliest studies of these two-way feedbacks was research by *Gutman et al.* [1984]. In this work, they defined a dryness index (based upon the ratio of annual net radiation to annual precipitation), which was used to infer the vegetation type at the land surface. A different magnitude of an index of water availability and the surface albedo were specified for different vegetation types. *Gutman* [1984] expanded this work by testing the sensitivity of the model to perturbations to the initial vegetation cover. He perturbed land surface conditions in different latitude belts to simulate deforestation, desertification, and irrigation of the tropical, semiarid, and desert zones, respectively. In all cases, perturbations to the biosphere were reflected in an altered atmospheric climate but not to the extent that the initial perturbations persisted. Gutman found that the impact of the biofeedback was strongest in the area adjacent to the perturbation zone, rather than within the perturbation zone itself.

Claussen [1994], utilizing asynchronous coupling, linked the equilibrium vegetation model, BIOME, to the European Center/Hamburg Model (ECHAM), the global climate model of the Max-Planck Institute for Meteorology. *Claussen* [1997] used an updated version of this model to test the sensitivity of equilibrium climate to perturbations in the initial vegetation state. In this study, he focused particularly on the African and Indian monsoon regions by replacing desert vegetation in these regions with rain forest vegetation and vice versa. He found that at equilibrium the forests had reasserted themselves on both continents at locations which had supported forests in the unperturbed simulation. Following a similar asynchronous coupling approach, *Texier et al.* [1997] coupled the Laboratoire de Météorologie Dynamique (LMD) atmospheric general circulation model (AGCM) to BIOME. Incorporation of vegetation feedbacks in simulations of the global climate 6000 B.P. was seen to strengthen the West African summer monsoon.

Gutman's [1984] and *Gutman et al.*'s [1984] studies are limited by the simplicity of the descriptions of different vegetation types and of the methodology for determining vegetation dominance. *Claussen*'s [1994, 1997] and *Texier et al.*'s [1997] work, while incorporating more physical realism, remain limited by the asynchronous coupling and the use of an equilibrium vegetation model to simulate the transient behavior of vegetation. *Levis et al.* [1997] and *Foley et al.* [1998] addressed many of the limitations of previous work by coupling the Integrated Biosphere Simulator (IBIS) to the Global Environmental and Ecological Simulation of Interactive Systems (GENESIS) AGCM. The structure of IBIS allowed fully synchronous coupling to the AGCM and includes a more complete description of plant competition and interaction with the atmosphere.

In this study, we continue this trend toward complete representation of the biosphere-atmosphere system with the development of a one-dimensional climate model which includes two-way interaction between the biosphere and the overlying atmosphere. Plant life responds to changes in atmospheric conditions, which are, in turn, influenced by biospheric conditions at the land surface. These changes in atmospheric conditions can then further influence vegetation at the land surface and so on in a potential feedback loop. Whether or not inclusion of ecosystem dynamics and these two-way feedbacks can result in multiple equilibria in the biosphere-atmosphere state is the subject of this study.

Our model is used to explore the response of the coupled system to perturbations to vegetation at the land surface. Specifically, our experiments investigate the possibility of multiple climate equilibria in tropical deforestation scenarios. We focus on the tropical forest region located near the coast of West Africa. We chose to use a one-dimensional framework for its simplicity and for its ability to isolate local effects from the effects of large-scale processes. Unlike other two-dimensional and three-dimensional studies, we can easily focus in on the processes in a particular region, without considering possible feedbacks with surrounding areas. However, because of the inherent limitations of a one-dimensional representation of a multidimensional system our model is not intended as a predictive tool. Rather, our model is intended to elucidate the processes and the constraints which may encourage or inhibit the development of multiple equilibria.

Following this introduction, section 2 describes our coupled model and each of its components. Section 3 outlines our experimental setup and also gives the results of our experimental simulations. Finally, section 4 presents the conclusions of this study.

2. Model Description

The model consists of several submodels coupled into a single integrated framework. The principal components of the integrated model are an atmospheric model, which includes representation of radiation and convection; a biospheric model, which includes vegetation dynamics; and a monsoon circulation model, which supplies the one-dimensional atmospheric column with horizontal fluxes of heat and moisture, allowing it to interact with its surroundings. Each of these components is described below.

2.1. Atmospheric Model

The atmospheric model is adapted from the one-dimensional model developed by *Renno* [1992]. It utilizes the radiation parameterizations developed by *Chou* [1986] and *Chou et al.* [1991] and the convection parameterization developed by *Emanuel* [1991]. The atmosphere is divided into 16 model layers, each 56 mbar thick, extending from the surface to $\sim$ 100 mbar. These layers are further subdivided in the radiation code. Above the layers explicitly simulated by the radiative-convective model the atmosphere is assumed to be in a state of radiative equilibrium. Incoming solar radiation at the top of the atmosphere is calculated on the basis of time and location, so that it includes both a diurnal and a seasonal cycle. Clouds are not explicitly represented in our model. Instead, we assume an atmospheric and cloud albedo of $\sim$ 25% and reduce the incoming solar radiation at the top of the atmosphere to reflect this atmospheric albedo. The value of the assumed albedo is fixed throughout the year and is chosen so that the mean annual solar radiation simulated at the surface approximates observations. While the effects of clouds on solar radiation are loosely represented in such a manner, the effects of clouds on longwave radiation are not considered.

Most processes in the coupled model are run at a 15-min time step. However, the timescale of radiative cooling is significantly longer, and thus we updated radiative tendencies only every 2 hours. This preserves the diurnal cycle in solar radiation while providing more computational efficiency.

The boundary layer of the atmosphere is represented in our model by assuming that the air and water vapor are well mixed. The temperature and specific humidity of the atmospheric layers included in the boundary layer are adjusted to satisfy this assumption at the end of each time step. There is no representation of the growth and decay of the depth of the boundary layer over the course of the day and the assumed depth does not vary with season. In these simulations we choose a boundary layer depth of 112 mbar as the best approximation of the actual depth of the boundary layer over forest conditions. Sensitivity tests have indicated that the atmospheric climate does not vary significantly for boundary layer depths between 60 mbar and 180 mbar.

2.2. Biospheric Model

We use IBIS version 1.1 as the biospheric component of our model. It incorporates all the components of a traditional soil-vegetation-atmosphere transfer (SVAT) model along with representations of plant growth and competition [*Foley et al.*, 1996]. In order to represent vegetation dynamics, nine plant functional types (seven trees types and two grass types) are defined on the basis of leaf form (broadleaf or needleleaf), leaf habit (evergreen or deciduous), and photosynthetic pathway (C3 or C4). Each plant functional type responds differently to climatic constraints which affect plant survival, and vegetation dynamics parameters describe their competitiveness for light and water. Their success in this competition can be measured by their leaf area index (LAI) and by their carbon biomass, both updated annually based on their net primary productivity (NPP) during that year.

The NPP of each plant functional type (PFT) is calculated as

$$NPP_i = (1-\eta)\int (A_{g,i} - R_{\text{leaf},i} - R_{\text{stem},i} - R_{\text{root},i})dt \tag{1}$$

where $A_{g,i}$ is the gross photosynthesis rate for the ith PFT, η is the fraction of carbon utilized for growth respiration and $R_{\text{leaf},i}$, $R_{\text{stem},i}$, and $R_{\text{root},i}$ are the maintenance respiration rates for leaves, stems, and roots, respectively.

The change in carbon storage C in reservoir j of PFT i is then given by

$$\frac{\partial C_{i,j}}{\partial t} = a_{i,j} NPP_i - \frac{C_{i,j}}{\tau_{i,j}}, \tag{2}$$

where $a_{i,j}$ represents the fraction of the annual NPP allocated to each carbon reservoir and $\tau_{i,j}$ is a turnover rate for carbon in each reservoir. The total biomass is simply the sum of carbon biomass in each reservoir. The LAI is obtained by dividing the carbon biomass in the leaves by the specific leaf area LAI_{spec}.

$$LAI_i = \frac{C_{i,\text{leaf}}}{LAI_{\text{spec}}} \tag{3}$$

In general, trees have first access to incoming solar radiation, shading the ground below them. Depending on the fractional coverage of the upper canopy (trees), the lower canopy (grasses) can receive very little sunlight for photosynthesis [*Larcher*, 1995]. This gives trees a competitive advantage when light is the primary object of competition. In the tropics this takes place when there is an abundant supply of water, and in these regions, forests are dominant.

As water becomes more scarce, water becomes the primary object of competition. While grasses, with

their shallower root structure, have first access to infiltrating water, trees have better access to deeper stores of soil water or groundwater. These differences are represented with different root profiles for different plant types. Different plant functional types also have different strategies for conserving water in times of scarcity. Drought deciduous trees, for example, are able to conserve water in times of water scarcity by dropping their leaves. Grasses, by dying back every year, can withstand a particularly long dry season. As the availability of water diminishes, vegetation in the tropics becomes sparser, transitioning from forest to savanna to grassland and, finally, to desert, as plants which are better able to obtain and conserve water become dominant.

The surface hydrology in IBIS was modified to account for spatial variability in interception loss and bare soil evaporation. These changes modified the partitioning of total evapotranspiration between interception loss, bare soil evaporation, and transpiration so that it was in closer agreement with observed values.

Spatial variability in precipitation tends to reduce spatially averaged interception loss [*Eltahir and Bras*, 1993a]. This reduction can be explained by two processes. First, spatial variability in precipitation concentrates intercepted water on a smaller wetted fraction of the canopy. Second, because the stored water is pooled in a smaller area, it has a greater depth and drains more quickly.

The first of these processes is addressed through modification of $F_{\max}$, the maximum wetted fraction of a leaf. We make the assumption that the rainfall which contributes to interception storage is distributed over a small fraction of the model domain. According to the method proposed by *Eltahir and Bras* [1993b], we further assume that the larger the rainfall amount, the larger this fraction, according to

$$F_{\max} = \frac{P}{P_{\text{climate}}}, \tag{4}$$

where P is the simulated precipitation and P_{climate} is the climatological average precipitation intensity for the region. P_{climate} is set at 2.6 mm/h and the maximum value of $F_{\max}$ is set at 1.0. The increased rate of drainage from the canopy with greater depth of storage is treated by decreasing T_{drip}, a decay time for the drainage of intercepted water.

We modified the IBIS representation of bare soil evaporation so that it considers spatial variability of the near-surface soil saturation. Following *Entekhabi and Eagleson* [1989], we assume a gamma distribution for the near-surface soil saturation and utilize this distribution in the calculation of bare soil evaporation.

2.3. Monsoon Circulation Model

When a one-dimensional model is used over land, water is continually lost from the system because of horizontal movement of surface and groundwater runoff and percolation of soil water into inaccessible groundwater storage. In order to keep the system from drying out, moisture must be supplied to the system in some manner. The simplest method is to prescribe a constant or time-varying amount of

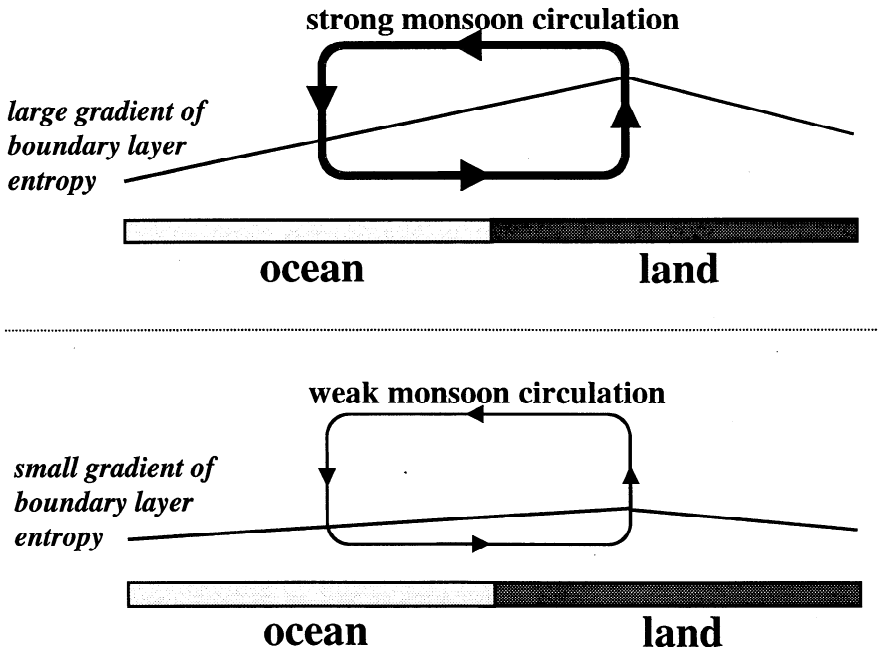

Figure 1. A strong gradient in boundary layer moist entropy is associated with a strong monsoon circulation. Conversely, a weak gradient in boundary layer moist entropy is associated with a weak monsoon circulation. After *Eltahir and Gong* [1996], reprinted by permission of the American Meteorological Society.

moisture convergence into the atmospheric column [*Koster and Eagleson,* 1990; *da Rocha et al.,* 1996]. However, the amount of moisture convergence has a strong effect on the modeled atmosphere, and as pointed out by *Brubaker et al.* [1991], atmospheric conditions simulated by the model are constrained by using a prescribed convergence. In using a one-dimensional model to simulate climate change, the simulated atmosphere should not be constrained to a limited range of equilibrium conditions by a prescribed convergence amount. Thus it is necessary to relate the amount of convergence into the column to conditions within the modeled domain, so that the simulated climate can evolve independently to any equilibrium.

Our monsoon circulation model assumes that the magnitudes of fluxes of air into and out of this region are related to the gradient in boundary layer moist entropy between the region and its surroundings, as depicted in Figure 1 [*Eltahir and Gong,* 1996]. A strong gradient in boundary layer moist entropy results in a strong monsoon and a large flux of air into a region. Conversely, a weak gradient in boundary layer moist entropy results in a weak monsoon circulation and a smaller flux of air. Boundary layer moist entropy is similar to other measures of near-surface conditions such as moist static energy. However, because boundary layer moist entropy is actually present in the governing equations for monsoon circulations, it is the most appropriate variable to use in the development of our model.

Eltahir and Gong [1996], using atmospheric circulation data from the Geophysical Fluid Dynamics Laboratory (GFDL), show that a larger gradient in boundary layer moist entropy is indeed associated with a stronger monsoon circulation in West Africa. Our own data analysis, using data from the National Centers for Environmental Prediction/National Center for Atmospheric Research (NCEP/NCAR) Reanalysis Project [*Kalnay et al.,* 1996], confirms this. Our model domain consists of a large column of air, and Figure 2 shows a plan view of the domain. It extends from 10°W to 7.5°E and 5°N to 10°N. An associated ocean region, also shown in Figure 2, extends from 10°W to 7.5°E and 1.25°S to 3.75°N. This ocean region is used to calculate the gradient in boundary layer moist entropy between the model domain and the nearby ocean.

Figure 3 shows the mass flux of air into the model domain from the south (across the 5°N boundary) and from the north (across the 10°N boundary). These fluxes are calculated using the meridional winds, integrated from 1000 mbar to 900 mbar. This corresponds roughly to the depth of our boundary layer. The fluxes are plotted against the entropy difference between the model domain and the ocean region to the south of the domain. Figure 3 was produced using 13 years of monthly data from the NCEP/NCAR Reanalysis Project.

The boundary layer moist entropy is an increasing function of both temperature and humidity. As seen

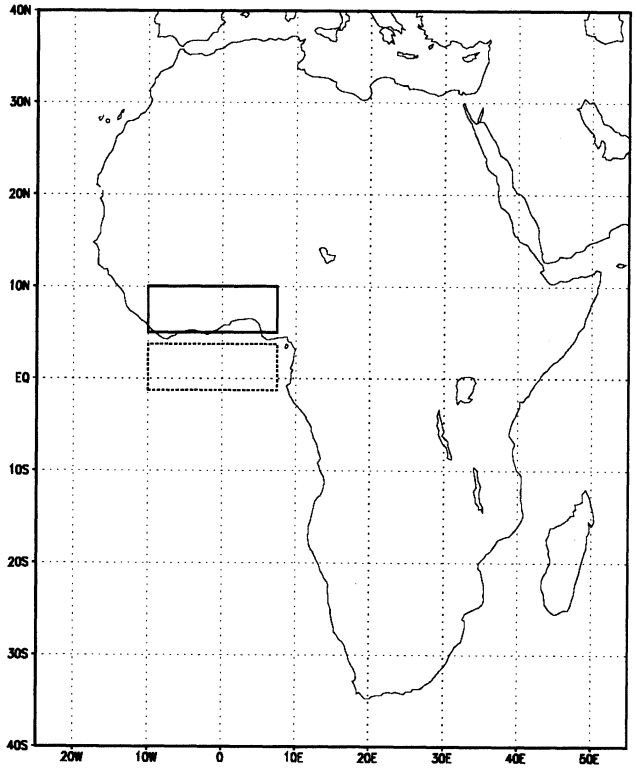

Figure 2. Our model domain consists of a single column of air whose horizontal extent is marked by the solid box shown here. The dotted box shows the ocean region used for the monsoon circulation model.

in Figure 4, the strength of the monsoon circulation in West Africa, as measured by the magnitude of the meridional fluxes of air, is better correlated with differences in boundary layer moist entropy between land and ocean than with differences in either temperature or specific humidity alone. In this domain, there is almost no correlation between temperature gradients and the strength of the monsoon circulation. While there is significant correlation between the gradient in specific humidity and the strength of the monsoon circulation, the difference in boundary layer moist entropy between land and ocean is a better indicator of the monsoon strength.

Using the data of Figure 3, we calibrated an empirical relation between the gradient of boundary layer moist entropy (between the land region and the ocean region) and the fluxes of air into the land region. Using this relationship, along with monthly climatological means of boundary layer moist entropy over the ocean and the model calculated boundary layer moist entropy over the model domain, we estimated the fluxes of air across the model boundaries.

Using these estimated fluxes, the moisture and heat advection into the region are calculated using a simple box model. The moisture tendency q_{tendency} is calculated for each level of the model atmosphere at each time step according to

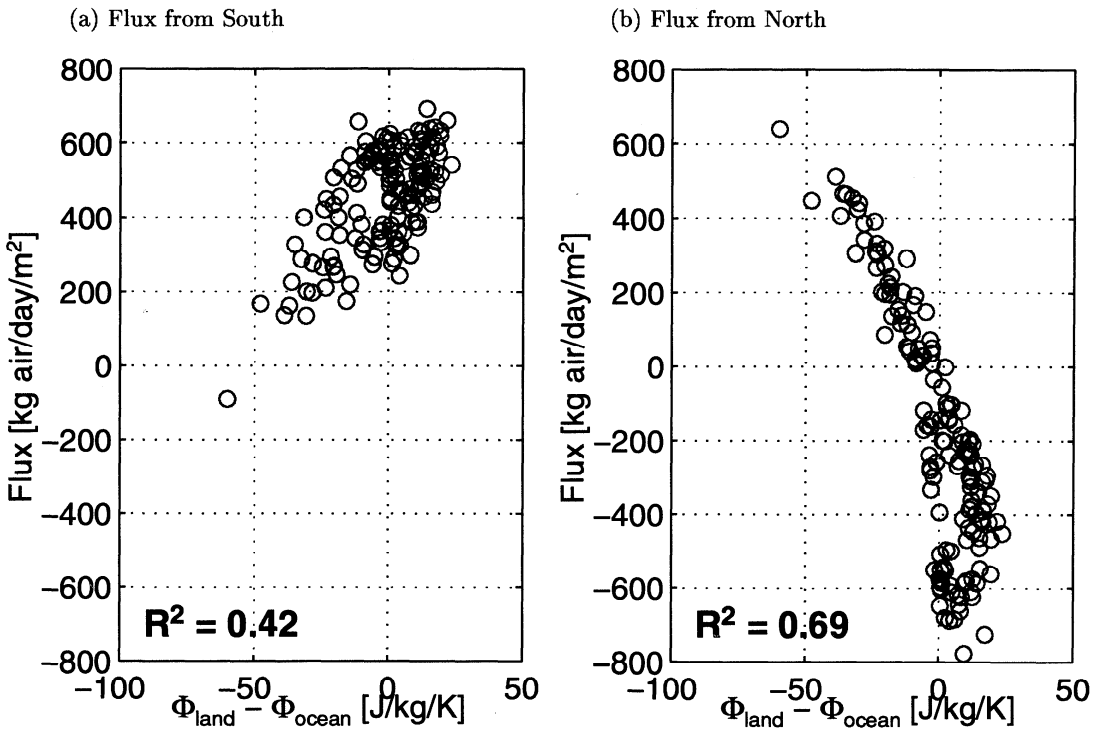

Figure 3. Mass fluxes of air into the model domain versus entropy difference between land and ocean. (a) Flux from south (across 5°N). (b) Flux from north (across 10°N).

$$q_{\text{new}} = \frac{q_{\text{advect}} M_{\text{advect}} + q_{\text{level}} M_{\text{level}}}{M_{\text{advect}} + M_{\text{level}}} \tag{5}$$

$$q_{\text{tendency}} = q_{\text{new}} - q_{\text{level}}, \tag{6}$$

where q_{new} is the new specific humidity of the model domain after horizontal advection of moisture has taken place, q_{advect} is the specific humidity of the advected air, and q_{level} is the current specific humidity of the model domain. M_{advect} is the mass of air which crosses into the domain during the time step, and M_{level} is the mass of air in one level of the model atmosphere. When M_{advect} is positive, air is brought into the model domain and q_{advect} takes on the value of the specific humidity of air at the domain boundary. Then q_{new} is the weighted average specific humidity of advected air and air within the domain. When M_{advect} is negative, flow is out of the domain, and q_{advect} takes on the same value as q_{level}. In this case, there is no net effect on the specific humidity within the model domain, and q_{tendency} equals zero. The temperature tendencies for each model level are calculated in the same manner.

Vertical velocities are deduced from the mass fluxes of air (M_{advect}) by assuming that the air is incompressible and applying the principle of conservation of air mass. The temperature and specific humidity tendencies due to vertical advection are calculated in a similar manner to the tendencies for horizontal advection.

3. Experimental Simulations

The same model domain described for the monsoon circulation model is used for three sets of experimental simulations. In each experiment the model is run at a 15-min time step, except for radiation, which is updated every 2 hours, vegetation phenology, which is updated daily, and vegetation dynamics, which are updated annually on the basis of growing conditions experienced during the preceding year.

3.1. Fixed Circulation Experiment

In the fixed circulation experiment, the monsoon circulation is fixed at its climatological intensity, as described by monthly NCEP/NCAR Reanalysis data.

3.1.1. Control simulation. In the control simulation, vegetation is initialized as mature forest, and we test the ability of the model to simulate a reasonable equilibrium vegetation and atmospheric climate from that starting point. In this simulation, the equilibrium vegetation is forest. Either deciduous or evergreen forest can exist in the region, depending on the initial conditions. In observations, the region from 5°N to 10°N actually consists of a mixture of evergreen forest, deciduous forest, and tall grass savanna at its northern edge. It is not unreasonable, then, for our model to simulate either forest type for the entire homogeneous region. Some of the characteristics of the

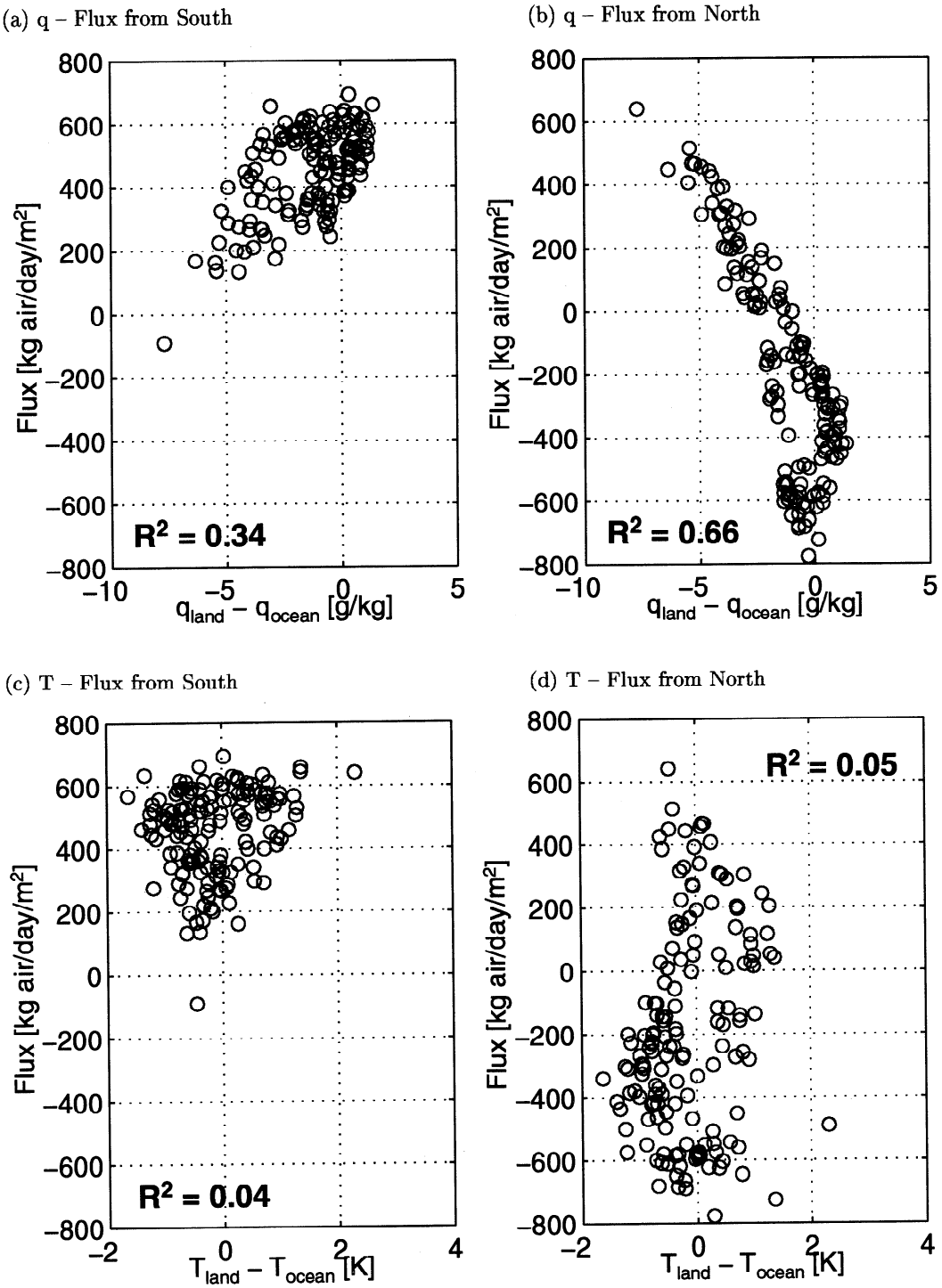

Figure 4. Correlation between mass flux of air and differences in specific humidity and temperature. (a) Specific humidity with flux from south (across 5°N). (b) Specific humidity with flux from north (across 10°N). (c) Temperature with flux from south (across 5°N). (d) Temperature with flux from north (across 10°N).

equilibrium vegetation are listed in Table 1. Typical observed values of these quantities for tropical forests are given in Table 2.

Although West Africa exhibits strong zonal symmetry, there are steep north-south gradients in both biospheric and atmospheric variables. Consequently, it is difficult to directly compare observational data to results from our large domain, which is assumed to be homogeneous. Our one-dimensional model is an abstraction of reality, including many simplifications

Table 1. Characteristics of the Equilibrium Vegetation in Each of Our Experiments.

	Net Primary Productivity, (NPP), kg C/m^2/yr	Biomass, kg C/m^2	Leaf Area Index, (LAI), m^2/m^2
Fixed circulation[a]	1.0	26	6.5
Interactive circulation	1.8	46	11.1
Modified circulation: Forest[a]	0.6	14	3.5
Modified circulation: Grass	1.1	2	8.4

[a] Values shown are for deciduous forest.

of the real world. Nevertheless, the average observed and simulated climates should bear resemblance to one another. Table 3 gives a comparison of the mean annual atmospheric climate of the fixed circulation control simulation, the NCEP/NCAR Reanalysis climatology for the region, and other observations of selected variables.

The annual average climate compares reasonably well with the climatology for the region, although the simulated climate is somewhat warmer and drier than observed. In terms of partitioning of water, precipitation and evaporation are in balance, and there is no runoff.

The partitioning of energy between latent and sensible heat fluxes is in good agreement with the observations. However, it should be noted that the sum of NCEP/NCAR's latent and sensible heat terms does not balance the net input of all-wave radiation at the surface reported by the same data set. The net solar radiation in our model closely approximates both the NCEP/NCAR and the International Satellite Cloud Climatology Project (ISCCP) climatological values, as the atmospheric albedo was tuned to give a similar incoming and net solar radiation to these data sets. Our model simulates a smaller net longwave radiation, resulting from both a higher simulated surface temperature and a smaller downward longwave radiative flux. The smaller downward longwave radiative flux is consistent with the drier atmosphere and lack of representation of cloud effects on longwave radiation.

The seasonal variability of the fixed circulation control simulation roughly approximates that seen in observations for most variables. Our precipitation and total evaporation show a summer maximum and winter minimum, consistent with observations for the region. The precipitation field shows good agreement with the NCEP/NCAR data and the Global Precipitation Climatology Project (GPCP) data [*Huffman*, 1997] for the same region during the dry season (Figure 5). However, our simulated summer peak reaches only $\sim$ 5 mm/d, compared to $\sim$ 6.5 mm/d in each of the other data sets.

Figure 5 also shows the boundary layer moist entropy in our model domain. Recalling that we will later make use of this quantity in estimating the monsoon strength, it is critical for us to simulate it well. As seen in Figure 5, the seasonal cycle of boundary layer moist entropy is simulated quite well by our coupled model when the monsoon is fixed at its climatological intensity. The seasonal distribution of specific humidity and temperature (not shown here) also match the NCEP/NCAR climatology fairly well when taken individually.

The seasonal variability in energy fluxes (not shown here) show reasonable agreement with the NCEP/NCAR and the ISCCP climatologies, with the exception of the solar energy field. Solar radiation is strongly affected by our lack of representation of variable cloud cover. The fixed cloud cover induces a seasonal bias in solar radiation, with higher intensity in the summer and lower intensity in the winter than is observed. Although this influences the energy fluxes in our model and also components of the water balance, the seasonal variability in our model simulation matches the seasonal variability in the NCEP/NCAR climatology fairly well, except in the solar radiation field.

Horizontal heat advection, especially latent heat advection, plays an important role in determining the

Table 2. Typical Values of NPP, Biomass, and LAI for Tropical Ecosystems.

	NPP, kg C/m^2/yr		Biomass, kg C/m^2		LAI, m^2/m^2	
	Range	Typical Value	Range	Typical Value	Range	Typical Value
Tropical evergreen forest	1-3.5	2	6-80	45	6-16	8
Tropical deciduous forest	1-3	1.5	6-60	40	6-10	-
Tropical grassland-savanna	≤ 2	1	0.2-15	4	1-5	-
Desert	≤ 0.2	-	≤ 4	-	≤ 1	-

Sources for data are: *Whittaker* [1975], *Lieth* [1973], and *Larcher* [1995].

Table 3. Simulated Mean Annual Climate of Control Simulations with Comparison to NCEP/NCAR Climatology and Observations

Variable	NCEP/NCAR Reanalysis Climatology[a]	Observations	Model Results	
			Fixed Circulation	Interactive Circulation
Temperature, K	299.7		301.8	300.6
Specific humidity, g/kg	16.4		12.6	13.5
Precipitation, mm/day	4.4	3.7[b]	3.4	4.5
Evapotranspiration, mm/day	3.4		3.4	4.3
Runoff, mm/day	1.1		0.0	0.2
Latent heat, W/m^2	99		99	125
Sensible heat, W/m^2	32		30	12
Net solar radiation, W/m^2	198	198[c]	204	201
Net longwave radiation, W/m^2	-57	-37[c]	-74	-68
Net all-wave radiation, W/m^2	141	162[c]	130	133
Boundary layer entropy, J/kg/K	5880		5860	5860

[a] NCEP/NCAR Reanalysis Data, 1982-1994 [*Kalnay et al.*, 1996].
[b] GPCP data, 1988-1997 [*Huffman et al.*,1997].
[c] ISCCP data, 1983-1991 [*Darnell et al.*, 1992].

seasonal climate of our model domain. The moisture advection is positive throughout most of the year but negative during the winter months.

Figure 6 shows the annual average atmospheric soundings of potential temperature and specific humidity for this control simulation. They are compared to NCEP/NCAR Reanalysis soundings. The potential temperature matches the NCEP/NCAR sounding quite well, except above 300 mbar, where our simulated temperature is much lower than that reported by NCEP/NCAR. The specific humidity also matches the NCEP/NCAR sounding well, except in the lowest 100 mbar of the atmosphere, where we have already noted that our simulations are drier than observations.

3.1.2. Grassland experiment: Static vegetation. In this experiment we test the sensitivity of the atmospheric climate to deforestation by simulating the equilibrium conditions reached when vegetation is fixed as grassland. The shift in the mean annual climate is relatively small, as shown in Table 4. Precipitation, total evaporation, and net all-wave radiation all decrease over grassland, while temperature decreases slightly following deforestation. The decrease in latent cooling (heating tendency) is slightly less than a compensating reduction in the net radiative input due to a change in surface albedo (cooling tendency), and thus the temperature is not greatly affected in our simulations.

3.1.3. Grassland experiment: Dynamic vegetation. When the model is initialized with grassland but vegetation dynamics are active so that both the biosphere and the atmosphere are free to find

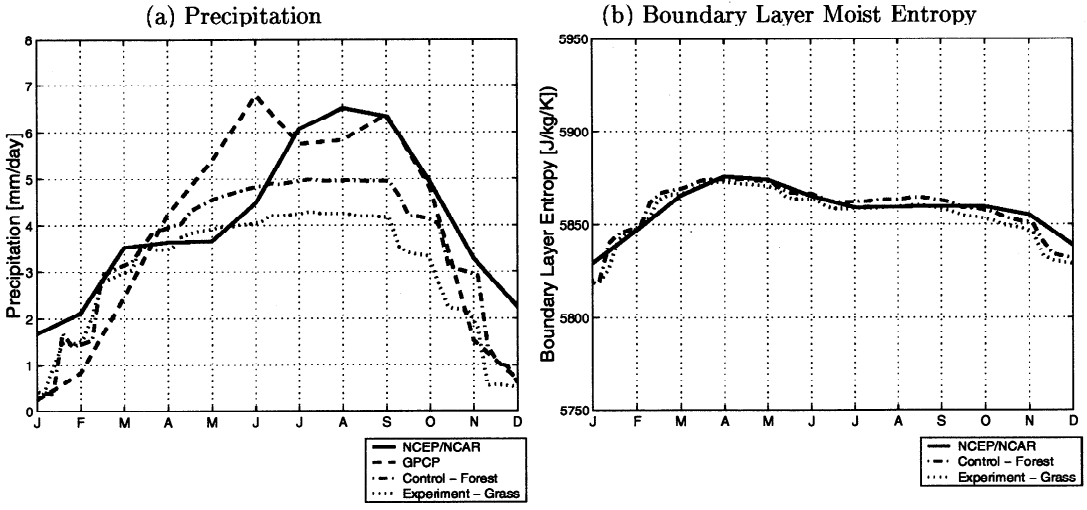

Figure 5. Seasonal cycle of (a) precipitation and (b) boundary layer moist entropy for fixed circulation experiment, compared to data from National Centers for Environmental Prediction (NCEP)/National Center for Atmospheric Research (NCAR) and Global Precipitation Climatology Project (GPCP).

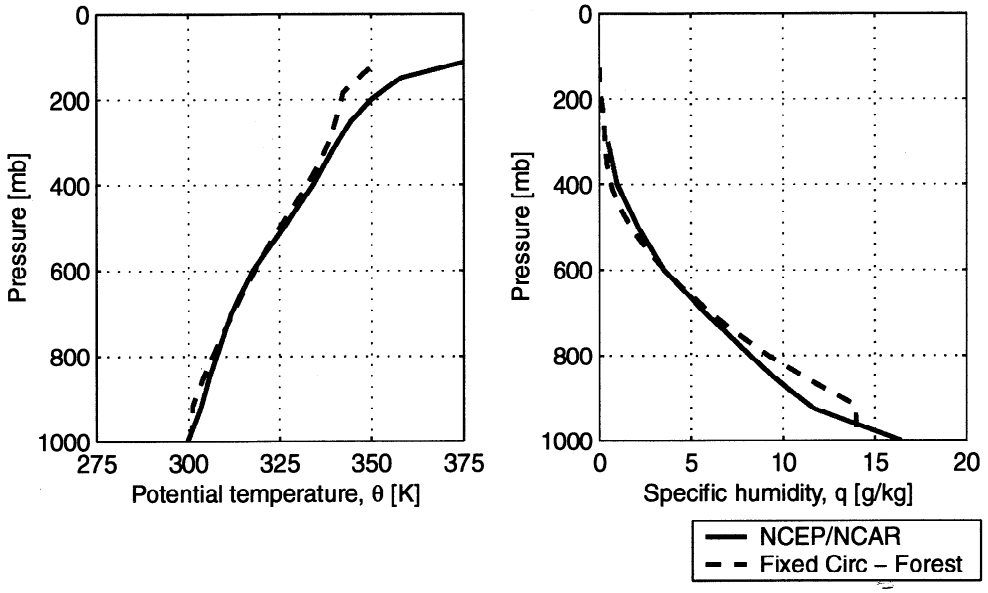

Figure 6. Atmospheric soundings, NCEP/NCAR versus fixed circulation control simulation.

their own equilibrium, we see that the grass quickly gives way to forest (Figure 7). The moderate change in climate does not prevent the regrowth of the forest.

Note that while the biomass takes many decades to stabilize, the LAI stabilizes much more quickly. When initialized with grassland, the forest LAI and NPP stabilize within $\sim$ 10 years at their equilibrium values of 6.5 and 1.0, respectively. It is the LAI which most directly impacts the competition between trees and grass, as it determines both the fractional coverage of the canopy and the area available to capture light. After the LAI has stabilized, biomass continues to increase while the trees grow taller and accumulate woody tissue.

3.2. Interactive Circulation Experiment

In the interactive circulation experiment the monsoon strength responds to local conditions, using the monsoon circulation model described in section 2.

3.2.1. Control simulation. In the control simulation, we initialize the vegetation as forest and allow the system to find its own equilibrium. The mean annual values of key variables at equilibrium are shown in Table 3 and compared to both observations for the region and the simulated atmospheric climate of the fixed circulation control simulation. The interactive circulation control simulation produced a somewhat moister and cooler climate than the fixed circulation control simulation. Precipitation exceeds evaporation, yielding 0.2 mm/d of runoff. The mean annual temperature and specific humidity are actually in closer agreement with the NCEP/NCAR climatology. Net solar radiation was essentially unchanged, but an increase in net longwave radiation brought the net all-wave radiation in closer agreement with observations. The change in net longwave radiation is largely due to the drop in surface temperature.

Table 4. Simulated Forest Versus Grassland Compared to Previous Modeling Studies of Amazonian Deforestation [a]

Study	Temperature, ΔT, K	Precipitation, ΔP, mm/day	Evaporation, ΔE, mm/day	Net Radiation, ΔRn, W/m^2
Lean and Warrilow [1989]	+2.0	-1.3	-0.6	n/a
Shukla et al. [1990]	+2.5	-1.8	-1.4	-26
Dickinson and Kennedy [1992]	+0.6	-1.4	-0.1	n/a
Henderson-Sellers et al [1993]	+0.6	-1.6	-0.6	n/a
Eltahir and Bras [1994]	+0.7	-0.4	-0.6	-13
Lean and Rowntree [1997]	+2.3	-0.3	-0.8	n/a
This study (fixed circulation)	-0.2	-0.3	-0.4	-21
This study (interactive circulation)	+0.4	-1.0	-0.9	-21
This study (modified circulation)	-0.6	-0.3	-0.3	-33

Here n/a indicates that data was not available.

[a] While strict comparisons should not be made because of the different locations of these studies, we can note that in almost all cases the sign of the changes in the listed variables are the same in our experiments and in the Amazonian deforestation experiments.

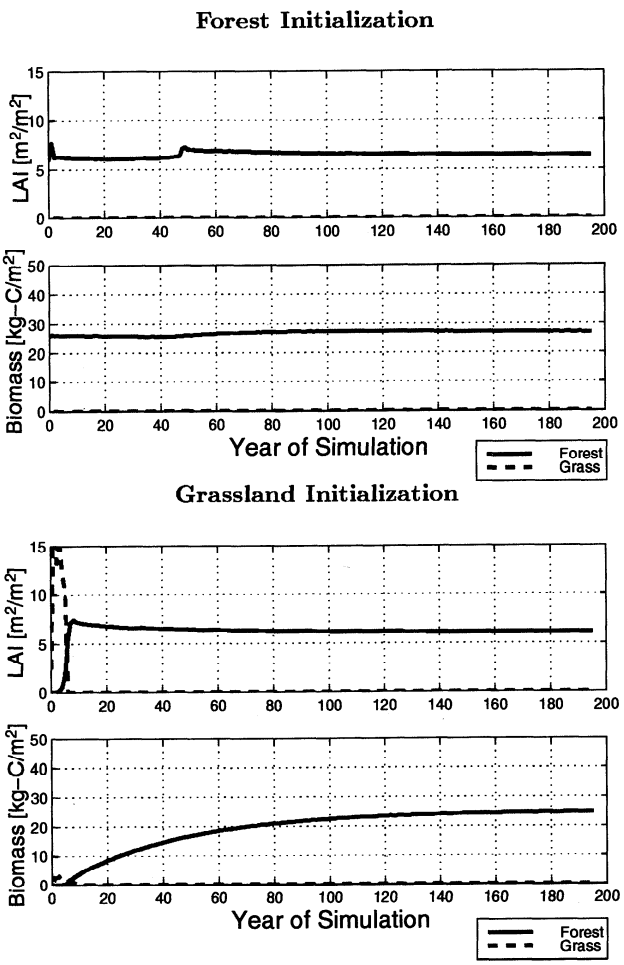

Figure 7. A single equilibrium vegetation state (represented by the leaf area index (LAI) and biomass of each vegetation type) is identified in our simulations using a fixed monsoon circulation, regardless of the initial vegetation condition.

Because of the wetter climate the equilibrium vegetation in this simulation is tropical evergreen forest. Deciduous forests are no longer competitive because they drop their leaves during the least productive months of the year, which correspond to those months with the driest soils. However, because there is plenty of water and not much seasonality, there is still adequate water during those months, and the trees would do better not to drop their leaves but instead to continue to photosynthesize during those months. Hence the evergreen forests become dominant in this simulation. The region sustains a tropical evergreen forest with an LAI of 11 and a biomass of 46 kg C/m^2/yr (see Figure 8 and Table 1). The NPP stabilizes at $\sim$ 1.8 kg C/m^2/yr. These values all lie within the range of observed values for tropical evergreen forests given in Table 2.

Although the mean annual climate in this simulation compares to the climatology for the region as well as or better than the mean annual climate in the fixed circulation control simulation, the seasonality of the climate in this simulation does not compare as well. In particular, the distributions of precipitation and boundary layer entropy (Figure 9), as well as other climatic variables, are flattened out in this simulation.

While the fluxes of air simulated by the monsoon circulation model do not match the climatological fluxes exactly, the simulated fluxes do capture the general seasonal trends observed in the NCEP/NCAR climatology (Figure 10). The surface flux across the southern domain boundary (5°N) remains positive throughout the year, consistent with the climatology. The mean annual surface wind speed of 2.7 m/s is in good agreement with the climatological wind speed. Furthermore, the magnitude of the seasonal variability in surface wind speed matches the climatology quite well, although winter winds are somewhat underestimated and fall winds are somewhat overestimated.

The winds at 10°N are not simulated as well. There is less seasonality in the simulated fluxes than observed in the climatology, reflected in the smaller amplitude of variability in the surface wind speed. The wind direction is almost always southerly (i.e., directed

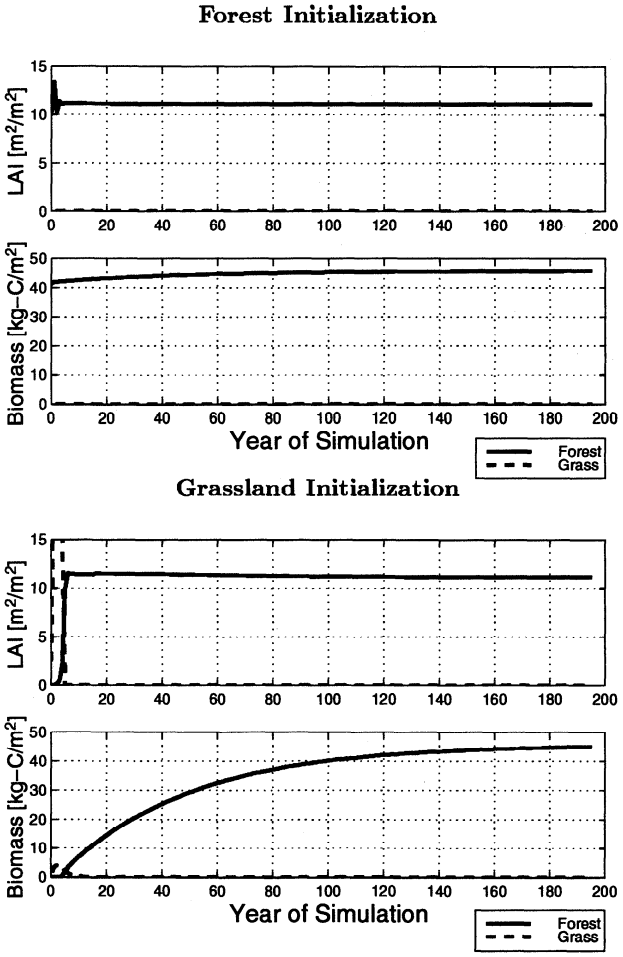

Figure 8. A single equilibrium vegetation state (represented by the LAI and biomass of each vegetation type) is identified in our simulations using an interactive monsoon circulation, regardless of the initial vegetation condition.

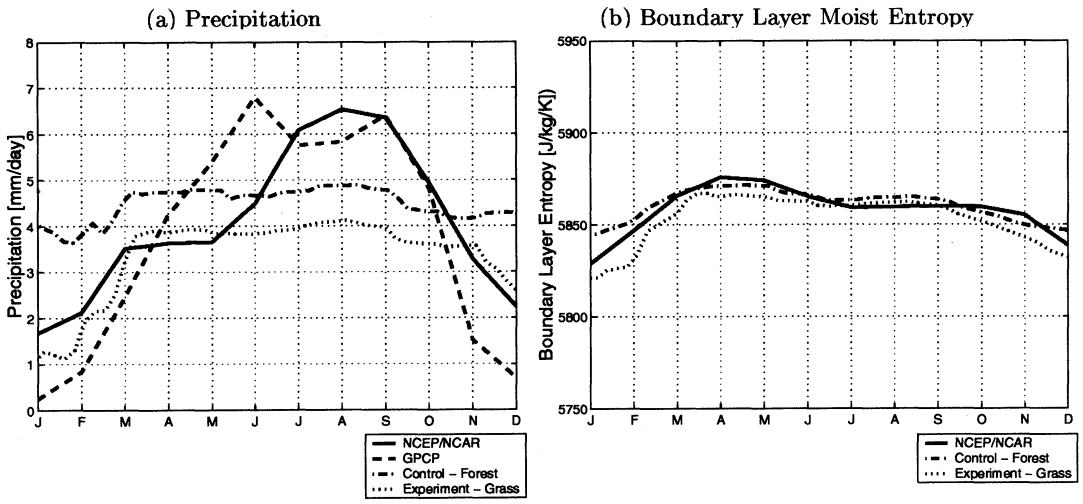

Figure 9. Seasonal cycle of (a) precipitation and (b) boundary layer moist entropy for interactive circulation experiment, compared to data from NCEP/NCAR and GPCP.

out of the domain) in this simulation. During the winter months the wind speeds drop and reverse briefly. However, these northerly winds are quite weak as compared to the climatology. Because of the diminished northerlies, there is less advection of hot dry air from the north into the model domain, and the simulated climate remains cooler and moister, with less seasonal variability.

Figure 11 shows the annual average atmospheric soundings of potential temperature and specific humidity for this control simulation alongside NCEP/NCAR Reanalysis soundings. As with the fixed circulation control simulation, the potential temperature matches the NCEP/NCAR sounding quite well. Again, our simulated atmosphere is colder than the NCEP/NCAR data at high elevation, but this effect is less pronounced in the interactive circulation simulation than in the fixed circulation simulation. The match between our simulated specific humidity profile and the NCEP/NCAR profile is within a few grams per kilogram, but as before, the simulation is drier in the lowest 100 mbar of the atmosphere.

3.2.2. Grassland experiment: Static vegetation. In this experiment the sensitivity of the atmospheric climate to vegetation change under an interactive monsoon circulation is tested by holding the vegetation fixed as grassland throughout the simulation. The sensitivity of the atmospheric climate to deforestation is greater than in the fixed circulation experiment. As seen in Table 4, precipitation and evaporation both decrease by $\sim$ 1 mm/d. Temperature increases slightly, by $\sim$ 0.4 K. The difference in net radiation of 21 W/m^2 reflects a smaller energy input to grassland than forest. The resulting climate has a

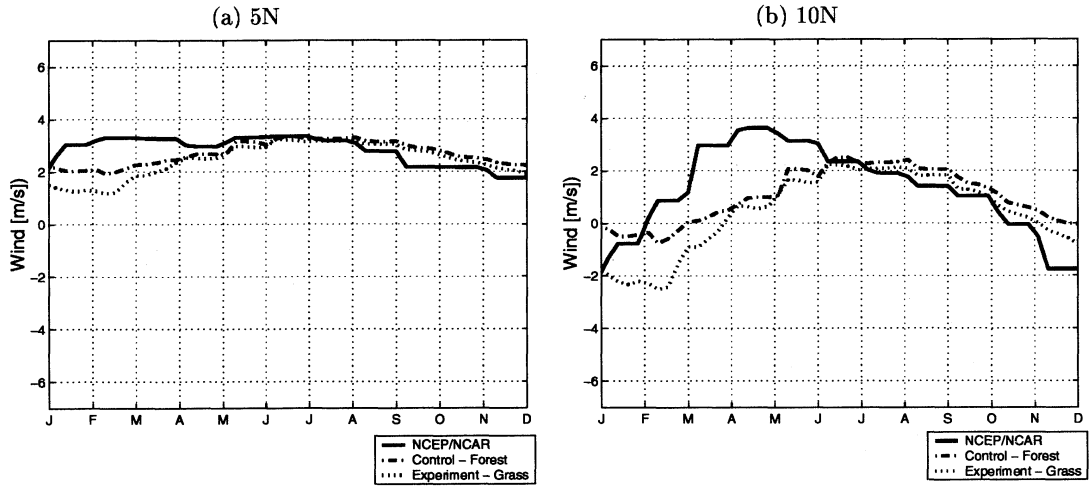

Figure 10. Seasonal cycle of simulated wind for interactive circulation experiment vs. data from NCEP/NCAR. (a) Meridional wind at 5°N (southern domain boundary). (b) Meridional wind at 10°N (northern domain boundary).

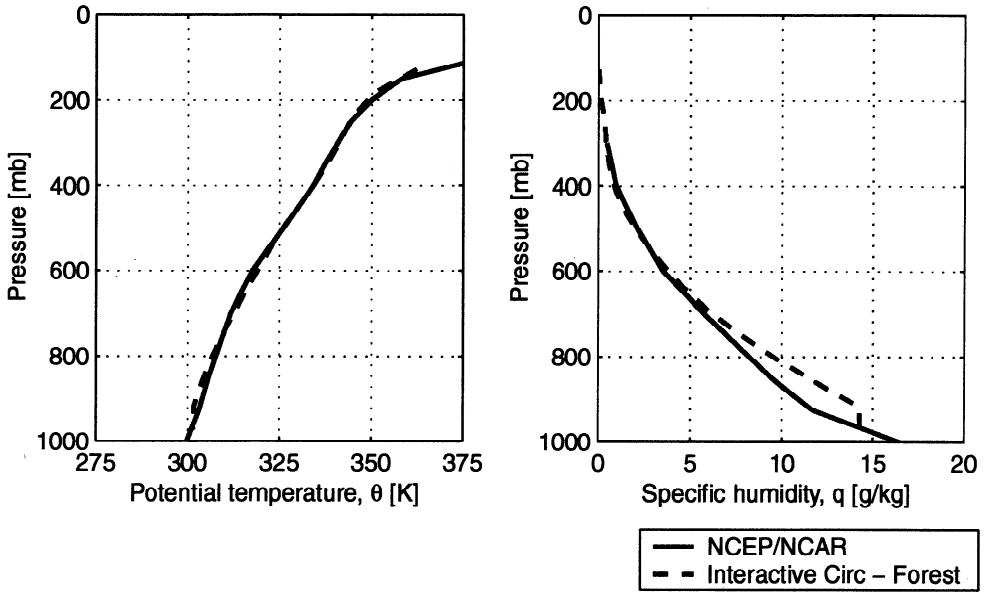

Figure 11. Atmospheric soundings, NCEP/NCAR vs. interactive circulation control simulation.

smaller boundary layer moist entropy and the monsoon circulation is consequently weaker under grassland conditions.

3.2.3. Grassland experiment: Dynamic vegetation. We then test for the possibility of multiple equilibria induced by vegetation change by initializing the vegetation as grassland and then allowing the coupled biosphere-atmosphere system to find its own equilibrium. Despite the large change in atmospheric climate with the change in vegetation, the equilibrium vegetation in the model domain reverts to forest. As seen in Figure 8, the vegetation has regained the LAI and NPP of the control simulation within $\sim$ 10 years. The biomass, while still accumulating, is approaching the same equilibrium point at the end of the simulation.

3.3. Modified Interactive Circulation Experiment

The model displays high sensitivity to the monsoon circulation model, especially to moisture advection at the northern boundary. As such, we explored this sensitivity further with simulations in which we modified the properties of the advected air at the northern boundary. Through use of the interactive monsoon circulation model the monsoon intensity varies with conditions in the model domain but transports air from a "degraded" region to the north. Instead of using the atmospheric properties observed at 10°N, the actual boundary, we used the atmospheric humidity and temperature profiles at 15°N to calculate horizontal moisture and heat advection. This mimics desertification in this adjacent region. In this experiment, we make just two simulations, one in which the vegetation is initialized as forest and one in which the vegetation is initialized as grassland. In both cases, vegetation dynamics are active and the climate is allowed to evolve toward its own equilibrium.

3.3.1. Forest experiment: Dynamic vegetation. When initialized with forest under the modified interactive circulation, the model simulates an equilibrium atmospheric climate which is substantially hotter and drier than was seen in the previous experiments. Annual average values for climatic variables are listed in Table 5.

In this simulation, precipitation drops to an annual average of 2.5 mm/d, just 55% of the precipitation seen in the interactive circulation control simulation. Evapotranspiration also decreases to 2.5 mm/d, and there is no runoff. The decrease in evapotranspiration results in a decrease in latent cooling of the near-surface air, and temperature increases by 2.7 K as compared to the control simulation. With a smaller latent heat flux, there is a compensating increase in the sensible

Table 5. Simulated Forest Versus Grassland for Modified Circulation Experiment

Variable	Modified Circulation (Profile at 15°N)	
	Forest	Grass
Temperature, K	303.3	302.7
Specific humidity, g/kg	9.8	9.1
Precipitation, mm/day	2.4	2.1
Total Evaporation, mm/day	2.4	2.1
Runoff, mm/day	0.0	0.0
Latent Heat, W/m2	70	61
Sensible Heat, W/m2	41	19
Net Solar, W/m2	206	187
Net Longwave, W/m2	-94	-108
Net Allwave, W/m2	112	79
Boundary layer entropy, J/kg/K	5840	5830

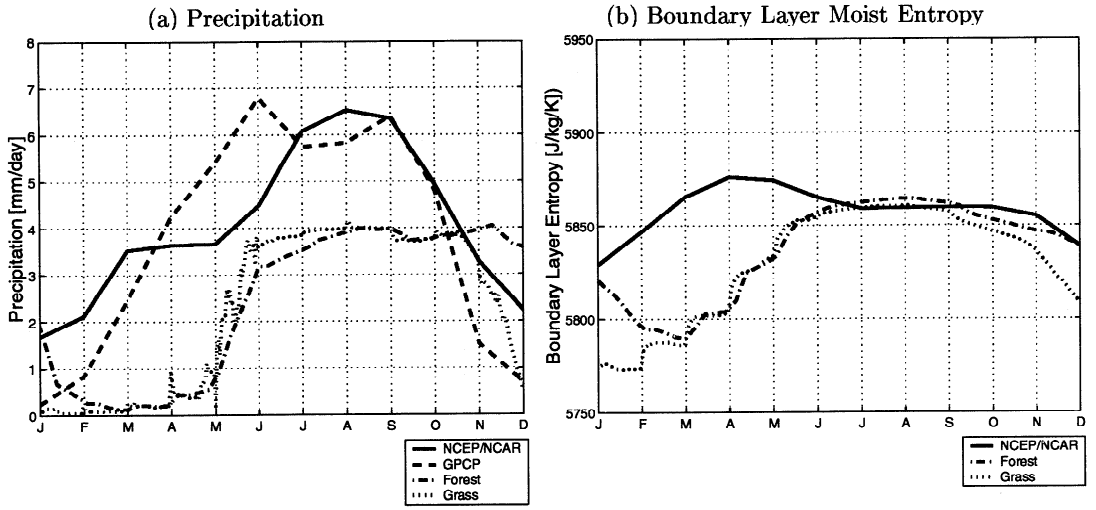

Figure 12. Seasonal cycle of (a) precipitation and (b) boundary layer moist entropy for modified circulation experiment, compared to data from NCEP/NCAR and GPCP.

heat flux of 29 W/m^2, and the Bowen ratio increases from 0.1 to 0.5. The outgoing longwave radiation increases because of the higher surface temperature, and the smaller atmospheric water content reduces the downward longwave radiative flux. The combination of these two effects decreases the net longwave radiation at the surface by 26 W/m^2. This is the main contribution to the 16% reduction in net all-wave radiation (from 133 W/m^2 to 112 W/m^2).

In addition to the change in mean annual climate, there is also a significant enhancement of seasonality with the modified profile of advected air. In particular, we may note a drier climate in the winter. Precipitation is < 1 mm/d from about February to the beginning of June (Figure 12). In contrast, there was little seasonality in precipitation in the interactive control simulation: it varied from ~ 4 mm/d in the winter to just under 5 mm/d in the summer. Correspondingly, the modified circulation simulation also shows strong seasonality in boundary layer moist entropy (Figure 12), evaporation, specific humidity, and temperature. In the dry season, during which total evapotranspiration is small, the decrease in latent cooling triggers a rapid rise in temperature to 310 K from a minimum of just under 300 K (not shown). The entropy range for this simulation is > 60 J/kg/K, as compared to a much more limited range of ~ 25 J/kg/K in the control simulation. With this variability in entropy also comes increased variability in the strength of the monsoon circulation. The surface wind across the southern boundary ranges from a minimum near 0 m/s in April to a maximum of ~ 3.5 m/s in September (Figure 13). In contrast, winds in the control simulation ranged from ~ 2 m/s to ~ 3.5 m/s. The surface wind speed across the northern boundary also shows greater seasonality and is directed into the domain (northerly) for 7 months of the year. In general, the monsoon circulation is seen to be much weaker in the winter than in the control simulation, consistent with the smaller boundary layer moist entropy.

The equilibrium vegetation for this simulation with diminished moisture and enhanced seasonality is forest (Figure 14). Either evergreen or drought deciduous trees are able to survive, depending on the initial condition. However, in either case, the forest has a small LAI of only 3.5. The stable NPP of 0.6 kg C/m^2/yr and biomass of 14 kg C/m^2 are each no more than one third that of the interactive circulation control simulation.

3.3.2. Grassland Experiment: Dynamic Vegetation. In this experimental simulation, vegetation is initialized with grassland conditions, and at equilibrium, grasses remain the dominant vegetation. As shown in Figure 14, the grass biomass remains stable at 2.2 kg C/m^2, with an NPP of 1.1 kg C/m^2/yr and an LAI of 8.4. The grassland climate is noticeably drier than the forest climate, as noted in Table 5. Precipitation and evaporation are 0.3 mm/d less than under forest cover, and the temperature is 0.6 K warmer.

4. Discussion and Conclusions

The one-dimensional model developed in this study is able to simulate the mean annual climatology and seasonality of coastal West Africa fairly well. It is also able to simulate most of the expected differences in atmospheric climate for grassland versus forest conditions. However, there was consistent bias in some fields. Very little runoff was generated in any of our simulations. A possible explanation for this is a lack of sufficient spatial and temporal variability. In our simulations, precipitation occurs every day during the wet season. Storms occur more frequently and with lesser intensity in our simulations, as compared to observations. This precipitation pattern tends to make surface runoff less likely, as precipitation reaching the

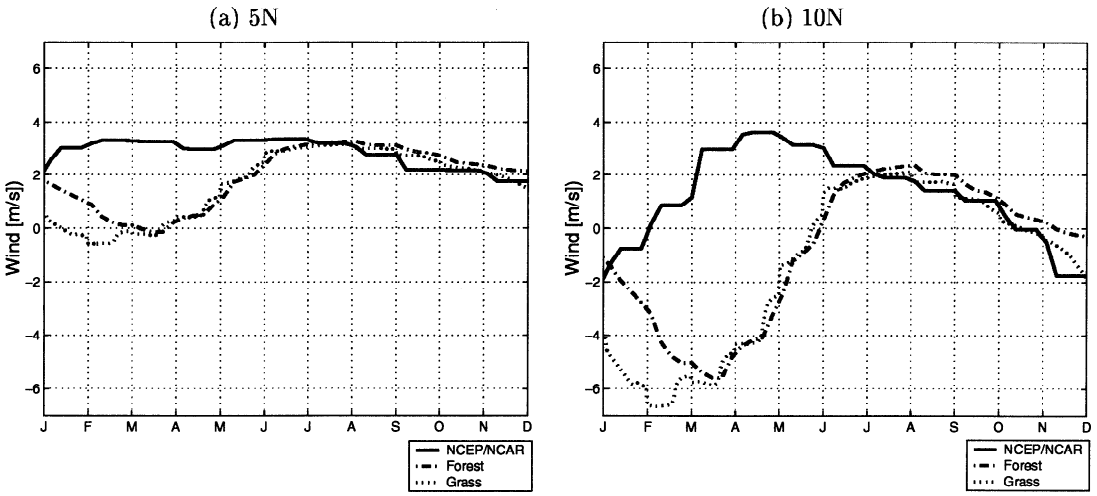

Figure 13. Seasonal cycle of simulated wind for modified circulation experiment versus data from NCEP/NCAR. (a) Meridional wind at 5°N (southern domain boundary). (b) Meridional wind at 10°N (northern domain boundary).

surface is less likely to exceed the infiltration capacity of the soil or to result in saturation of the uppermost layers of soil. It may also tend to inhibit subsurface runoff as smaller infiltration fronts stay closer to the surface where plants have access to the stored soil moisture. Further changes to the surface hydrology module to incorporate spatial variability, such as was done for interception loss and soil evaporation, should improve the match between simulated runoff and observed runoff.

The solar radiation field was also biased because of the lack of representation of variable cloud cover. Although this bias did not carry over to significantly bias any other fields, addition of variable cloud cover should improve the model's ability to simulate actual conditions in West Africa.

Other problems which were noted earlier in the text include the flattened seasonality of the interactive circulation control simulation, which arises due to error in the wind magnitudes simulated by the monsoon circulation model. Clearly, there are limitations to our simple one-dimensional model. While it cannot capture every detail of the actual conditions in coastal West Africa, it does simulate conditions well enough to draw some useful conclusions.

Our monsoon circulation model illustrates the possibility of feedbacks caused by the monsoon circulation itself. Using a modified interactive monsoon circulation, we simulated a much weaker monsoon circulation than in the unmodified case. The weaker circulation allowed more hot and dry air from the north into the model domain, further reducing the energy of air in the model domain and thus further weakening the monsoon. This feedback becomes more important under the modified monsoon circulation because the advected air (profile at 15°N) is less energetic than the advected air in the control simulations (profile at 10°N). This result suggests that climatic conditions in regions adjacent to the model domain are critical to the determination of climate within the model domain itself. The importance of interactions with neighboring regions was also noted by *Gutman* [1984].

Our simulations also indicate that the strength of the monsoon circulation has a strong affect not only on the atmospheric climate but also on the state of the biosphere. The equilibrium forest vegetation under the fixed monsoon circulation, interactive monsoon circulation, and modified interactive monsoon circulation were all different. A stronger monsoon with less wintertime intrusion of hot and dry winds from the north was able to sustain a more healthy forest, as measured by LAI and biomass.

Our experiments provide some insight into vegetation dynamics and the conditions necessary for multiple equilibria in the biosphere-atmosphere system to exist. In the fixed circulation experiments, forest was found to enjoy a stable equilibrium in our model domain. Recalling that the relative abundance of water is what controls the competition between trees and grasses in this region, we may note that the mean annual precipitation decreases by only 0.3 mm/d with grassland versus forest cover. Thus forest is able to recover after an initial specification of grassland.

In our interactive circulation experiments, we noted a 1 mm/d drop in annual average precipitation when forest was replaced by grassland. However, despite this relatively large drop in water availability, the magnitude of the precipitation remains more than sufficient to support a full canopied forest, and we again see a stable forest equilibrium.

With a modified interactive circulation, the possibility of two different equilibria arises. When initialized with forest, atmospheric conditions are barely able to sustain a forest. When the domain

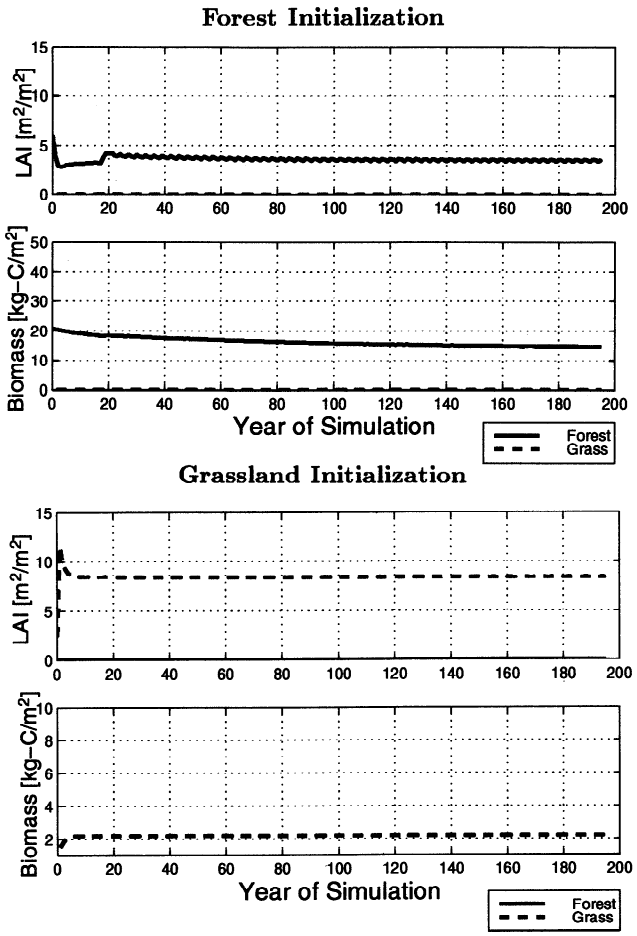

Figure 14. With a modified circulation due to degraded conditions to the north, our simulations indicate the possibility of multiple equilibria, depending on the initial vegetation state (represented here by LAI and biomass).

is initialized with grassland, however, the diminished moisture availability prevents the recovery of forest, and grasses prevail. With the weakened monsoon and diminished precipitation, there is insufficient moisture to support forest. When moisture availability falls below a certain threshold, the resource competition shifts to one in which water is the limiting resource. In this case, grasses which are better able to exploit soil moisture in the wet season and conserve moisture in the dry season are able to outcompete trees.

When the system is initialized with forest vegetation under the modified interactive circulation, there is just enough precipitation for trees to maintain a full canopy and thus exclude grasses on the basis of competition for light. Thus, although the NPP and LAI of the equilibrium forest are actually smaller than that of the equilibrium grassland, it is by virtue of the fact that there is just enough water to support a full canopy that the forest is able to dominate.

The precipitation under grassland conditions is only 0.3 mm/d less than that under forest conditions. This small change is sufficient to move the system to a new equilibrium because the precipitation amount lies near the threshold defining the dominance of grass versus trees. In the simulations with fixed monsoon circulation or unmodified interactive monsoon circulation, changes in precipitation of the same or greater magnitude did not result in a change in the equilibrium climate because the system was not positioned near this threshold.

To summarize, our experiments with three different specifications of the monsoon circulation suggest the following conclusions.

1. The monsoon circulation plays an important role in the modulation of climate, as indicated by the two different equilibria in our fixed circulation and interactive circulation experiments. The feedbacks between the biosphere and atmosphere involving the monsoon circulation are important in determining the equilibrium climate.

2. Our experiments with the fixed monsoon circulation and the interactive monsoon circulation suggest that the forest ecosystem along the coast of West Africa is quite stable to most of the perturbations that are likely to occur due to vegetation changes. Given enough time, forests can ultimately recover in this region. However, the size of the trees and the health of the ecosystem does depend on the availability of water, as indicated by the different biomass, LAI, and NPP under different precipitation regimes.

3. The state of adjacent regions is seen to have significant impacts on the monsoon circulation and the regional climate system. The change in the northern boundary conditions produced a much drier, hotter, and more seasonal climate which was able to support less dense vegetation than the control climate. While forest is a possible equilibrium in this modified circulation experiment, the size and density of the trees are much smaller than in either the fixed circulation or interactive circulation experiments. Here again, we see that the health of the forest depends heavily on the availability of water.

4. When the biosphere-atmosphere system is initialized with grassland under a modified circulation, forest is unable to recover. Grassland becomes dominant even though the magnitude of the change in water availability is relatively small. The existence of multiple equilibria in the vegetation-climate system depends not only on the absolute magnitude of the perturbation to climate but also on whether or not the perturbation pushes the climate over a threshold in moisture conditions which defines the dominance between two different vegetation types. Systems which lie near such a threshold will be more likely to give rise to multiple equilibria in the vegetation-climate system.

The importance of the monsoon circulation in determining climate and the importance of the state of surrounding areas suggests that two-dimensional and three-dimensional modeling work can give additional insight into biosphere-atmosphere interactions in monsoonal regions.

While our work suggests that multiple equilibria will not exist in very humid areas such as near

the coast of West Africa, it does not suggest that biosphere-atmosphere interactions are unimportant in such regions. As long as changes to the land cover are sustained through continued use as ranchland or other nonforest uses, the climatic impacts of land cover changes will be felt and the magnitude of that climatic shift remains important.

Acknowledgments. This research was supported by NASA agreements NAGW-5201, NAG5-7525, and NAG5-8617 and by NSF agreement ATM 9807068. The views, opinions, and/or findings contained in this paper are those of the authors and should not be construed as an official NASA or NSF position, policy, or decision, unless so designated by other documentation. In addition, one author was supported by an NSF graduate research fellowship, an NSF traineeship in the Hydrologic Sciences, a Ralph M. Parsons Fellowship, and a Global Climate Modelling Initiative Fellowship. Some components of the model developed in this study were provided courtesy of Nilton Renno of the University of Arizona and Jonathan Foley and his group at the University of Wisconsin, Madison. Their advice during the development of the model is much appreciated.

References

Brubaker, K.L., D. Entekhabi, and P.S. Eagleson, Atmospheric water vapor transport: Estimation of continental precipitation recycling and parameterization of a simple climate model, *Tech. Rep. 333*, 166 pp., Ralph M. Parsons Lab., Mass. Inst. of Technol., 1991.

Chou, M.-D., Atmospheric solar heating rate in the water vapor bands, *J. Clim. Appl. Meteorol., 25*, 1532-1542, 1986.

Chou, M.-D., D.P. Kratz, and W. Ridgway, Infrared radiation parameterizations in numerical climate models, *J. Clim., 4*, 424-437, 1991.

Claussen, M., On coupling global biome models with climate models, *Clim. Res., 4*, 203-221, 1994.

Claussen, M., Modeling bio-geophysical feedback in the African and Indian monsoon region, *Clim. Dyn., 13*, 247-257, 1997.

Darnell, W., et al., Seasonal variation of surface radiation budget derived from International Satellite Cloud Climatology Project C1 data, *J. Geophys. Res., 97*, 15,741-15,760, 1992.

da Rocha, H.R., et al., A vegetation-atmosphere interaction study for Amazonia deforestation using field data and a 'single column' model, *Q. J. R. Meteorol. Soc., 122*, 567-594, 1996.

Dickinson, R. E., and P. Kennedy, Impacts on regional climate of Amazon deforestation, *Geophys. Res. Lett., 19*, 1947-1950, 1992.

Eltahir, E. A., Role of vegetation in sustaining large-scale atmospheric circulations in the tropics, *J. Geophys. Res., 101*, 4255-4268, 1996.

Eltahir, E. A., and R. L. Bras, A description of rainfall interception over large areas, *J. Clim., 6*, 1002-1008, 1993a.

Eltahir, E. A., and R. L. Bras, Estimation of the fractional coverage of rainfall in climate models, *J. Clim., 6*, 639-644, 1993b.

Eltahir, E. A., and R. L. Bras, Sensitivity of regional climate to deforestation in the Amazon basin, *Adv. Water Resour., 17*, 101-115, 1994.

Eltahir, E. A., and C. Gong, Dynamics of wet and dry years in West Africa, *J. Clim., 9*, 1030-1042, 1996.

Emanuel, K. A., A scheme for representing cumulus convection in large-scale models, *J. Atmos. Sci., 48*, 2313-2335, 1991.

Entekhabi, D., and P. Eagleson, Land surface hydrology parameterization for atmospheric general circulation models including subgrid scale spatial variability, *J. Clim., 2*, 816-831, 1989.

Foley, J. A., et al., An integrated biosphere model of land surface processes, terrestrial carbon balance, and vegetation dynamics, *Global Biogeochem. Cycles, 10*, 603-628, 1996.

Foley, J. A., et al., Coupling dynamic models of climate and vegetation, *Global Change Biol., 4*, 561-579, 1998.

Gutman, G., Numerical experiments on land surface alterations with a zonal model allowing for interaction between the geobotanic state and climate, *J. Atmos. Sci., 41*, 2679-2685, 1984.

Gutman, G., G. Ohring, and J. H. Joseph, Interaction between the geobotanic state and climate: A suggested approach and a test with a zonal model, *J. Atmos. Sci., 41*, 2663-2678, 1984.

Henderson-Sellers, A., et al., Tropical deforestation: Modelling local to regional scale climate change, *J. Geophys. Res., 98*, 7289-7315, 1993.

Huffman, G., et al., The global precipitation climatology project (GPCP) combined precipitation dataset, *Bull. Am. Meteorol. Soc., 78*, 5-20, 1997.

Kalnay, E., et al., The NCEP/NCAR 40-year reanalysis project, *Bull. Am. Meteorol. Soc., 77*, 437-471, 1996.

Koster, R., and P. Eagleson, A one-dimensional interactive soil atmosphere model for testing formulations of surface hydrology, *J. Clim., 3*, 593-606, 1990.

Larcher, W., *Physiological Plant Ecology*, 3rd ed., Springer-Verlag, New York, 1995.

Lean, J., and P. R. Rowntree, Understanding the sensitivity of a GCM simulation of Amazonian deforestation to the specification of vegetation and soil characteristics, *J. Clim., 10*, 1216-1235, 1987.

Lean, J., and D. Warrilow, Simulation of the regional climatic impact of Amazon deforestation, *Nature, 342*, 411-413, 1989.

Levis, S., and J. A. Foley and D. Pollard, Sensitivity of a synchronously coupled dynamic model of climate and vegetation to the choice of initial vegetation conditions (abstract), *Eos Trans. AGU, 78(46)*, Fall Meet. Suppl., F260, 1997.

Lieth, H., Primary production: Terrestrial ecosystems, *Hum. Ecol., 1*, 303-332, 1973.

Meher-Homji, V., Effects of forests on precipitation in India, in *Forests, Climate, and Hydrology: Regional Impacts*, edited by E. R. C. Reynolds, and F. B. Thompson, pp. 51-77, United Nations Univ., Tokyo, 1988.

Renno, N. D. O., Cumulus convection parameterization and numerical modeling of moist atmospheres, Ph.D. thesis, Mass. Inst. of Technol., Cambridge, 1992.

Shukla, J., and C. Nobre, and P. Sellers, Amazon deforestation and climate change, *Science, 247*, 1322-1325, 1990.

Texier, D., et al., Quantifying the role of biosphere-atmosphere feedbacks in climate change: Coupled model simulations for 6000 years BP and comparison with palaeodata for Northern Eurasia and Northern Africa, *Clim. Dyn., 13*, 865-882.

Whitakker, R. H., *Communities and Ecosystems*, 2nd ed., MacMillan, Indianapolis, 1975.

Zheng, X., and E. A. Eltahir, The role of vegetation in the dynamics of West African monsoons, *J. Clim., 11*, 2078-2096, 1998.

E. A. B. Eltahir MIT 48-207 Cambridge, MA 02139 (e-mail: eltahir@mit.edu)

J. E. Kiang MIT 48-208 Cambridge, MA 02139 (e-mail: jkiang@mit.edu)

(Received March 29, 1999; revised June 29, 1999; accepted July 29, 1999.)